CHALMERS
UNIVERSITY OF TECHNOLOGY

Cross-layer static resource provisioning for dynamic traffic in flexible grid optical networks

Citation for the original published paper (version of record):
Xu, Y., Agrell, E., Brandt Pearce, M. (2021). Cross-layer static resource provisioning for dynamic traffic in flexible grid optical networks. Journal of Optical Communications and Networking, 13(3): 1-13. http://dx.doi.org/10.1364/JOCN.404693

(article starts on next page)

Cross-layer Static Resource Provisioning for Dynamic Traffic in Flexible Grid Optical Networks

YUXIN XU[*1,3], ERIK AGRELL[2], AND MAITE BRANDT-PEARCE[3]

[1] College of Information Engineering, Zhejiang University Of Technology, Zhejiang, China, 310000
[2] Department of Electrical Engineering, Chalmers University of Technology, SE-41296 Gothenburg, Sweden
[3] Charles L. Brown Department of Electrical and Computer Engineering, University of Virginia, Charlottesville, Virginia 22904, USA
[*] Corresponding author: yx4vf@virginia.edu

Compiled November 19, 2020

Flexible grid networks need rigorous resource planning to avoid network over-dimensioning and resource over-provisioning. The network must provision the hardware and spectrum resources statically, even for dynamic random bandwidth demands, due to the infrastructure of flexible grid networks, hardware limitations, and the reconfiguration speed of the control plane. We propose a flexible-online-offline probabilistic (FOOP) algorithm for the static spectrum assignment of random bandwidth demands. The FOOP algorithm considers the probabilistic nature of random bandwidth demands and balances hardware and control plane pressures with spectrum assignment efficiency. The FOOP algorithm uses the probabilistic spectrum Gaussian noise (PSGN) model to estimate the physical-layer impairment (PLIs) for random bandwidth traffic. Compared to a benchmark spectrum assignment algorithm and a widely applied PLI estimation model, the proposed FOOP algorithm using the PSGN model saves up to 49% of network resources.

http://dx.doi.org/10.1364/jocn.XX.XXXXXX

1. INTRODUCTION

With the development of modern communication technology, flexible grid networks have become a promising solution to overcome shortages in network resources. Flexible grid networks efficiently utilize the spectrum by partitioning it into many finely grided frequency slots (6.25 GHz or 12.5 GHz) [1–3]. However, network resources such as spectrum, transceivers, and switches are costly and energy-consuming considering the constantly increasing communication traffic. Efficient network resource provisioning is essential for establishing future flexible grid networks. A robust cross-layer network resource provisioning approach needs to have three main components: a valid traffic model, an efficient yet scalable resource assignment algorithm, and an accurate physical layer model.

The increasingly heterogeneous traffic is geographically and temporally dependent on traffic data-rates that can vary significantly within hours [4]. In current dense wavelength division multiplexed (DWDM) optical networks, time-varying traffic does not severely impair the spectrum utilization because of the coarse 50 GHz frequency grid [1]. However, for flexible grid networks, heterogeneity does matter. Most provisioning approaches do not consider the time-varying nature of the traffic that has a random data-rate, and simply use the maximum bandwidth of the traffic, referred to in this paper as *standard provisioning*. Utilizing standard provisioning is an appropriate solution for DWDM networks, but it is not efficient for flexible grid networks. Migrating the algorithms designed for DWDM networks to flexible grid networks without considering the implications due to the finer grid is wasteful, and often results in significant over-provisioning [3, 5, 6].

In addition, traffic comes from various applications with different latency requirements. For example, some traffic, such as autonomous driving data, remote control, and real-time voice services, require low traffic latency. However, large-volume data backup between data centers is not very latency-sensitive. Resource provisioning algorithms can exploit such differences in requirements.

For realistic continental-scale optical backbone networks, the resource provisioning algorithm has to satisfy the following requirements: (a) the algorithm should be non-disruptive and long-term stable for established connections; (b) the network accessibility must be robust and reliable; (c) the algorithm should not be too conservative to prevent resource over-provisioning [3, 7].

Offline resource allocation algorithms satisfy requirements (a) and (b). These algorithms are suitable for traffic that is slowly time-varying (months or years) and can thus be considered deterministic. Offline algorithms are also referred to as static algorithms due to the reasons mentioned above, and traditionally configure the traffic by its maximum bandwidth needed to provide high robustness. These less time-sensitive algorithms pre-assign fixed spectrum and routing, and the control plane executes the pre-planned results by assigning the traffic with fixed resources [3, 7]. Therefore, requirement (c) above is not satisfied by conventional offline algorithms because they tend to be over-conservative and lack flexibility.

On the contrary, online algorithms are considered dynamic because they deal with fast-varying traffic in real-time or within a short time delay (minutes or hours). These algorithms easily meet requirements (b) and (c) because the resources (routing and spectrum) are assigned flexibly by the control plane in one or a few time periods with respect to the actual network state (traffic volume, signal quality, control plane load and other metrics of the network). However, online algorithms are significantly less stable due to the frequent changes in established connections, and can thus add substantial pressure to the control plane and hardware infrastructure [3].

In recently proposed offline resource provisioning algorithms for time-varying traffic [3, 8–10], time is considered an extra optimization dimension. These algorithms perform a flexible resource allocation based on a highly-scalable dynamic resource assignment while considering the comprehensive interests of multiple consecutive time periods (overall interests within the time frames). In [10], the proposed algorithm employs this approach using integer linear programming (ILP) with time-varying traffic between time periods. It also proposes an elastic-spectrum allocation to prevent wasting spectrum resources. However, this algorithm causes much network disruption, which requires more advanced hardware and results in a heavy computational burden [3, 7].

In [8, 9], the authors proposed using the statistical network assignment process (SNAP) algorithm based on Monte Carlo simulations to obtain the expected network state. The traffic's data-rate is randomly selected in each simulation trial (also considered as a time period), and then network resources are assigned by a static network planning algorithm for the randomly-selected traffic state. After obtaining all simulated time periods, the hardware infrastructure, e.g., regeneration resources (regeneration nodes and circuits), are then assigned statically. This algorithm requires an astronomically large number of simulation trials to obtain all possible network states when the problem dimension is large and requires extremely massive computational resources.

In this paper, which extends our preliminary work [11], we propose a flexible online-offline probabilistic (FOOP) combined resource provisioning algorithm. The FOOP algorithm is a routing, spectrum, and regeneration assignment (RSRA) algorithm. It considers the randomness of the demands' bandwidth as an extra optimization dimension instead of considering time as the extra dimension. Time-varying traffic is modeled in a probabilistic way, and thus the network resources (spectrum) are also assigned probabilistically. With the probabilistic information about the traffic, the overall network resources can be aggressively planned to prevent over-provisioning. The FOOP algorithm provides a comprehensive solution with respect to all traffic scenarios without depending on time periods. The complexity of the FOOP algorithm is as low as a single trial of SNAP. Therefore, it is able to address the resource allocation problem for continental-scale networks in which every node has data transmission to every other node.

Furthermore, taking into account the probabilistic nature of heterogeneous traffic, instead of conservatively reserving resources for rare scenarios (always reserving spectrum for the maximum bandwidth that may be needed), the FOOP algorithm avoids resource over-provisioning by aggressively assigning network resources to common scenarios. It then addresses the rare scenarios when the bandwidth exceeds the provisioned spectral allocation by a compensation mechanism. Our proposed FOOP algorithm saves considerable spectrum usage.

Due to the nature of realistic traffic, some demands are more resource-consuming than others (bottlenecks of resource provisioning); we refer to these as resource-consuming (RC) demands. The others we refer to as low-resource-consuming (LRC) demands. In this research, RC demands are planned by the offline algorithm, and LRC demands are assigned by an online algorithm. Through this design, the FOOP algorithm balances the aforementioned requirements (a), (b), and (c). The offline part provides non-disruptive and stable light-paths with a carefully planned network resource assignment to the bulk of the traffic. The online part for the remaining LRC demands adds flexibility to the resource assignment and significantly reduces the complexity.

The standard Gaussian noise (GN) model is one of the simplest and most popular physical-layer impairment (PLI) estimates, but it is not suitable for estimating the PLIs of random bandwidth traffic [12, 13]. In [5], we propose a probabilistic spectrum Gaussian noise (PSGN) model based on the GN model to optimize the regeneration resource deployment for long-haul optical networks. The PSGN model is suitable for random bandwidth traffic and results in simple closed-form equations. How conservative the algorithm is in estimating the noise level (the margin between the actual noise and the noise estimated by PSGN for random bandwidth demands) is selectable by the network designer. Unlike the widely applied transmission reach (TR) based PLI estimate [6, 14], which estimates the worst-case PLIs, the GN-based PSGN model is network-state dependent and thus provides higher accuracy and remarkable resource savings. We show through simulation that using the proposed PSGN model saves almost half of the regeneration resources needed compared to using the TR model.

We envision the FOOP algorithm using the PSGN model as an integral part of dynamic and heterogeneous optical networks of the future. It can provide network operators with information about spectrum reserves that operators can use opportunistically. They may even be able to lease their precious spectrum resources to other operators while still preserving their data transmission requirements [15, 16].

This paper is organized as follows. In Section 2, we introduce the proposed FOOP algorithm. Section 3 then describes the proposed PLI model, the PSGN model. Section 4 presents the regeneration resource deployment scheme for long-haul optical networks. Section 5 provides our simulation setting, numerical results, and analyses. Finally, we draw conclusions in Section 6.

2. FLEXIBLE-ONLINE-OFFLINE PROBABILISTIC ALGORITHM

We envision a software-defined network (SDN) as shown in [Fig. 3, 17] and [Fig. 7, 7]. The SDN control layer sends instructions to the network infrastructure via OpenFlow [17]. Centralized

SDN controllers realize network functions such as routing and demand accommodations [7, 17]. The FOOP algorithm is embedded in the SDN controllers in the control layer to efficiently accommodate network resources.

The FOOP algorithm utilizes probabilistic information about the traffic to accommodate bottleneck demands aggressively. It can be applied to networks using any routing algorithm, such as shortest-path. In order to add flexibility to the network, the FOOP algorithm provisions spectral resources for smaller demands through an online approach.

The FOOP algorithm aggressively assigns a static spectrum to random bandwidth traffic in order to avoid network disruption (relieving hardware and control plane pressure) but still saving spectral resources. Instead of reserving the maximum spectrum that may be needed for each demand, the spectrum (or guard-bands) allocated to adjacent demands is allowed to overlap slightly with a low probability of occurrence. When the spectrum assigned to two adjacent demands overlaps because the demands experience large bandwidths at the same time, the portion of the signal in the overlapped spectrum may be corrupted.

The resulting rare spectral overlap can have different effects on different network designs. In classical networks with large guard-bands between channels, the idea of placing adjacent channels with low probability of occurrence closer simply reduces the size of these margins. In marginless or low-margin networks, the signal in the potentially overlapped spectral region must be pre-processed (pre-filtered and a collision warning generated) to avoid corruption, and it may become distorted. For sliced spectrum wavelength-division multiplexing (WDM) optical networks [18], this intentional spectrum overlap is manageable and almost harmless. In these networks, multiple independent 2.5-10 Gb/s sub-channels are groomed and transmitted as super-channels of $\geq$ 40 Gb/s [18]. Due to the independence between sub-channels, a collision of two super-channels only corrupts the sub-channels on the edges that overlap; the non-overlapped sub-channels are not corrupted. In orthogonal frequency-division multiplexing (OFDM) based optical networks [1] that comprise independent sub-carriers for data transmission, the impact of spectral overlap is similar. When a spectrum collision occurs, only overlapping sub-carriers are corrupted; the remaining non-overlapping sub-carriers are not affected. For the rare occurrence of a traffic collision, the control plane can easily compensate for the loss of data by re-transmission. A clever network control system may place latency insensitive sub-channels at the outer edges of the spectrum, in case a re-transmission is necessary. For networks catering to broadband single-carrier signals, signal processing may be used to correct the signal distortion caused by spectral overlap or over-filtering, as was suggested in [19].

A. Demand Statistics and Partitioning

For the proposed RSRA algorithm, FOOP, we assume the cumulative distribution function (CDF), $F_{\Delta_q}(\delta)$, and the maximum bandwidth, $B_q = \max \operatorname{supp} \Delta_q$, of the random bandwidth Δ_q are known for demand $q \in \mathbb{D}$, where $\mathbb{D}$ represents all demands that need to be served in the network. In Section 5C, we consider the case when the CDF is not fully known or inaccurately estimated.

As described in Section 1, traffic is categorized into RC and LRC demands. The FOOP algorithm comprises two stages: 1) an offline resource provisioning algorithm for the RC demands and 2) an online assignment for the LRC demands, as shown in Algorithm 1. RC demands deserve to be aggressively provisioned in order to maximally save limited network resources. LRC demands can be assigned by our online algorithm after executing the offline algorithm in order to utilize the fragmented network resources.

In RSRA algorithms, the network resources consumed (spectrum usage and regeneration resource) by a demand q correlate with the route distance ℓ_q and the maximum bandwidth B_q for demand $q \in \mathbb{D}$. Hence, we propose a multi-term cost function for prioritizing the allocation of demands on the network,

$$H(q) = \varpi \ell_q + \chi B_q, \tag{1}$$

where ϖ and χ are weighting parameters for balancing the factors. Utilizing (1), demands are sorted and categorized as either RC or LRC and then offered as the input to either the offline or online algorithm, described below. $\mathbb{D}_{RC}$ and $\mathbb{D}_{LRC}$ represent the sets of RC and LRC demands, respectively, where $\mathbb{D} = \mathbb{D}_{RC} \cup \mathbb{D}_{LRC}$. Once the demands have been partitioned, the algorithm performs the offline and online steps, successively. By changing the weighting parameters, $H(q)$ emphasizes a different priority of network resources and hence obtains different orders of demands and different elements in $\mathbb{D}_{RC}$ and $\mathbb{D}_{LRC}$, which impacts the results of the RSRA algorithms.

B. Offline Resource Provisioning

The offline provisioning algorithm contains three steps, shown in Algorithm 2, to assign resources to the demands categorized as resource-consuming. This algorithm is a generalization of the approach given in [11]. First, a routing and spectrum assignment (RSA) is performed: demands are routed by a desired routing algorithm (we use the shortest-path algorithm for our results), and then a probabilistic spectrum assignment is employed for the random-bandwidth RC traffic. Second, having obtained the RSA, the PSGN model is then used to predict the extent of PLIs for the random bandwidth demands. Third, an optimal mixed integer linear program (MILP) [14] uses the estimate of the PLIs to optimally assign the regeneration nodes and circuits in the network.

The traffic can be routed through any stand-alone algorithm (not performed jointly with the spectrum assignment), such as the widely-applied shortest-path algorithm, which is very computational friendly. As is well known, the shortest-path algorithm trades off the complexity and performance (as measured by the resources used). In this research, we do not explore the effect of diverse routing schemes on network resource usage since this topic has been well studied [3, 20]. The route (ordered set of nodes or links) for demand q is denoted as $\mathcal{U}_q$.

The probabilistic spectrum assignment attributes a frequency range and determines a spectrum occupancy distribution within this range on the light-path for each demand $q \in \mathbb{D}_{RC}$. For every possible bandwidth realization δ, a starting frequency $f_q^{\text{start}}(\delta)$ within the spectrum assigned for q is determined by step 1 in Algorithm 2 based on the spectrum assignment scheme used. Note, $f_q^{\text{start}}(\delta)$ denotes the lowest frequency assigned to q when $\Delta_q = \delta$. This algorithm operates on any spectrum allocation scheme. For the numerical results in this paper, we use the first-fit spectrum assignment due to its scalability.

The offline portion of the FOOP algorithm assigns spectrum aggressively by exploiting the probability that a frequency f is occupied by demand q on link l, denoted as $S_{q,l}(f)$, as shown in Figure 1. Let $I_{q,l}(f) \in \{0, 1\}$ denote the presence of demand q on link l at frequency f; then $\Pr[I_{q,l}(f) = 1] = S_{q,l}(f)$ represents demand q's occupancy probability, i.e., $S_{q,l}(f) = \Pr[f_q^{\text{start}}(\Delta_q) \leq$

Algorithm 1. Flexible Online-Offline Combined Probabilistic Algorithm

Input: Demands $q \in \mathbb{D}$ with known bandwidth statistics F_{Δ_q}; network topology with a set of links $\mathbb{L}$ and nodes $\mathbb{N}$; network parameters $\mathbb{F}$ as listed in Table 1; spectrum overlapping probability threshold B.

Definitions: The network is modeled as a connected graph $(\mathbb{N}, \mathbb{L})$ where a node is denoted by $n \in \mathbb{N}$ and a unidirectional link $l \in \mathbb{L}$. $\mathbb{U}$ is the routing data for the input demands; $U_q \in \mathbb{U}$ is the route for a demand $q \in \mathbb{D}$; $\mathbf{H}$ is the vector of costs for the input demands with elements $H(q)$; subscripts RC and LRC represent the sets of RC demands $\mathbb{D}_{RC}$ and LRC demands $\mathbb{D}_{LRC}$, respectively; $\mathbb{C}$ is the spectrum allocation for the demands, where $\mathbb{C}_{LRC} \cup \mathbb{C}_{RC} = \mathbb{C}$; $\mathbb{U}_{RC}$ and $\mathbb{U}_{LRC}$ are the routes for demand sets $\mathbb{D}_{RC}$ and $\mathbb{D}_{LRC}$, respectively; $\mathbb{G}_{RC}$ is the estimate of PLIs of the RC demands, derived in Section 3; $\mathbb{T}$ is the regeneration nodes and circuits assignment, described in Section 4. For network planning, define $\mathbb{B}$ as the set of maximum bandwidths B_q for all demands q; for network operation, define $\mathbb{B}$ as the set of actual bandwidths δ_q for all demands q.

procedure FOOP ALGORITHM($\mathbb{D}, \mathbb{L}, \mathbb{N}, B, \mathbb{F}$)

I. Routing:

Perform the shortest-path algorithm on all demands $\mathbb{D}$:

Obtain the routing data $\mathbb{U}$ for $\mathbb{D}$

II. Sorting:

Calculate demands cost by $H(q) = \varpi \ell_q + \chi B_q$

Categorize demands into $\mathbb{D}_{RC}$ and $\mathbb{D}_{LRC}$ based on descending ordered elements of $\mathbf{H}$:

Obtain $\mathbb{D}_{RC}$ and $\mathbb{D}_{LRC}$

III. Spectrum assignment:

procedure OFFLINE PROBABILISTIC ALGORITHM($\mathbb{D}_{RC}$, $\mathbb{L}, \mathbb{N}, B, \mathbb{F}$)

Obtain $\mathbb{U}_{RC}$, $\mathbb{C}_{RC}$, $\mathbb{G}_{RC}$, and $\mathbb{T}$

end procedure

procedure ONLINE ASSIGNMENT($\mathbb{D}_{LRC}$, $\mathbb{U}_{RC}$, $\mathbb{C}_{RC}$, $\mathbb{L}, \mathbb{N}, \mathbb{F}, \mathbb{B}$)

Obtain $\mathbb{U}_{LRC}$ and $\mathbb{C}_{LRC}$

end procedure

end procedure

Output: $\mathbb{U}_{RC}$, $\mathbb{U}_{LRC}$, $\mathbb{C}_{RC}$, $\mathbb{C}_{LRC}$, $\mathbb{G}_{RC}$, and $\mathbb{T}$

$f \le f_q^{\text{start}}(\Delta_q) + \Delta_q]$. Depending on the CDF of the bandwidth, $S_{q,l}(f)$ could have long low-probability tails.

We propose to aggressively assign spectrum to demands so that there is a small probability B of overlap between adjacent connections' reserved spectrum. Recall that spectrum collisions only influence the spectral guard-bands or overlapped sub-channels while keeping the data transmission of non-overlapping signals intact. In the likely case that overlapping does not happen, all the data are successfully transmitted. P_l^{OL} represents the overlapping probability at frequency f on link l:

$$P_l^{\text{OL}}(f) = \Pr[\sum_{q, l \in U_q} I_{q,l}(f) > 1]$$
$$= 1 - \prod_{q, l \in U_q} S_{q,l}(f) - \sum_{q, l \in U_q} \left(S_{q,l}(f) \prod_{x \neq q} [1 - S_{x,l}(f)] \right). \quad (2)$$

where x represents adjacent demands sharing the same link with demand q.

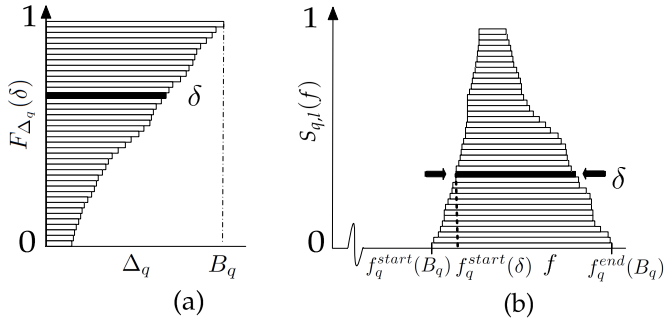

Fig. 1. (a) CDF of bandwidth of demand q. (b) Frequency occupancy distribution $S_{q,l}(f)$ of demand q.

In order to achieve reliable and robust data transmission, we design the offline algorithm so that for each link l, $P_l^{\text{OL}}(f) \le B, \forall f$. This condition allows a limited spectrum assignment overlap.

Once the routing and spectrum assignments are executed, the PSGN model is used to provide a noise estimate $\mathbb{G}_{RC}$, where the PLIs of all demands $q \in \mathbb{D}_{RC}$ are estimated. The PSGN model first described in [5] is accurate at estimating the PLIs of random bandwidth traffic. It is also able to estimate the PLIs in scenarios with non-zero probability of intentional spectrum collisions. To account for spectral collisions, and using (2), the spectrum occupancy probability at frequency f for other demands $x \neq q$ on link l can be written as

$$\hat{P}_{q,l}(f) = \Pr[\hat{I}_{q,l}(f) = 1] = \Pr[\sum_{x \neq q} I_{x,l}(f) \ge 1] \quad (3)$$
$$= 1 - \prod_{x \neq q} [1 - S_{x,l}(f)], \quad (4)$$

where $\hat{I}_{q,l}(f) \in \{0, 1\}$ is the indicator that denotes the occupancy of frequency f by at least one other channel sharing link l with demand q. $\hat{P}_{q,l}(f)$, which measures the probability that a frequency point f has been re-utilized (assigned multiple times because of frequency overlap) for other demands sharing the same link with the channel of interest q, is needed to calculate the PLIs in step 2 of Algorithm 2. This is described below in Section 3.

As shown in step 3 of Algorithm 2, after estimating the PLIs for all demands, an MILP algorithm described below in Section 4 is applied to optimally and globally deploy regeneration nodes to guarantee the transmission quality.

C. Online Assignment

After carefully and aggressively assigning resources using probabilistic provisioning for the bottleneck RC demands, an online assignment is designed for the LRC demands, shown in Algorithm 3. These LRC demands are routed by a desired routing algorithm (the shortest-path algorithm) with a standard first-fit spectrum assignment, shown in step 1 in Algorithm 3. Because these remaining random bandwidth demands do not require many resources, assigning these demands by an online method rarely causes disruption. Moreover, these demands do not add significant PLIs because they are either small in bandwidth or short in transmission distance. Assigning these demands by the online algorithm adds flexibility and prevents wasting fragmented network resources. Therefore, the online assignment enhances the efficiency of resource utilization.

Algorithm 2. Offline Probabilistic Algorithm [11]

Input: resource-consuming demands $\mathbb{D}_{RC}$; network topology with a set of links $\mathbb{L}$ and nodes $\mathbb{N}$; network parameters $\mathbb{F}$; spectrum overlapping probability threshold B.

Definitions: Same as for Algorithm 1. In addition, $f_q^{\text{start}}(\delta)$ denotes the lowest frequency assigned to demand $q \in \mathbb{D}_{RC}$ when $\Delta_q = \delta$; $\mathbb{C}_{RC}$ comprises $f_q^{\text{start}}(\delta)$ for all bandwidths $\delta \in \text{supp}\,\Delta_q$ and all $q \in \mathbb{D}_{RC}$.

procedure OFFLINE PROBABILISTIC ALGORITHM($\mathbb{D}_{RC}$, $\mathbb{L}, \mathbb{N}, B, \mathbb{F}$)

1. Route demands $\mathbb{D}_{RC}$ using any desired routing algorithm:

Obtain the routing data $\mathbb{U}_{RC}$ for $\mathbb{D}_{RC}$

for each $q \in \mathbb{D}_{RC}$ **do**

Based on U_q, use first-fit to find $f_q^{\text{start}}(B_q)$, where $S_{q,l}(f)$ satisfies $P_l^{\text{OL}}(f) \le B$, $\forall f, l$.

end for

Obtain the spectrum assignment $\mathbb{C}_{RC}$ for $\mathbb{D}_{RC}$

2. Use the PSGN model for PLI estimation:

Obtain the noise estimation $\mathbb{G}_{RC}$

3. Based on $\mathbb{D}_{RC}$, $\mathbb{G}_{RC}$, and $\mathbb{U}_{RC}$, use MILP to assign the regeneration nodes:

Obtain the regeneration assignment $\mathbb{T}$

end procedure

Output: $\mathbb{U}_{RC}$, $\mathbb{C}_{RC}$, $\mathbb{G}_{RC}$, and $\mathbb{T}$

The online assignment algorithm is invoked in two modes: network operation and network planning. In network operation, the bandwidths δ_q of all demands q are known and input to Algorithm 3. In network planning, however, only the statistics of the random bandwidths are known, and their maximum values B_q are input to Algorithm 3, as captured by parameter $\mathbb{B}$.

3. MODELING PLI FOR AN OVERLAPPED SPECTRUM ASSIGNMENT

Long-haul optical networks require an accurate PLI estimation algorithm so that the quality of transmission (QoT) for demands is guaranteed. In this paper, we make the following assumptions for modeling PLIs to calculate $\mathbb{G}_{RC}$, which consists of $G_{q,l} \in \mathbb{G}_{RC}$ for each $q \in \mathbb{D}_{RC}$ and $l \in \mathbb{L}$. We consider a dual-polarization transmission scheme with the same modulation format and the same power spectral density (PSD) in both polarizations. We adopt similar assumptions as in [14, 21]. Several main types of PLIs are taken into account: nonlinear distortion, chromatic dispersion, and amplified spontaneous emission (ASE) noise [12]. Modern digital signal processing techniques are able to compensate for chromatic dispersion. Thus we only consider the impairments of the nonlinear interference (NLI) due to the interaction of nonlinearity and dispersion in the fiber and ASE noise due to the erbium-doped fiber amplifiers [14, 21]. We assume that the PLIs consist of additive noise and interference (assumed independent), accumulating incoherently over all spans on the transparent segment. In this paper, we consider the widely applied transmission reach (TR) model as the benchmark. The TR model is conservative and estimates the worst-case noise for demands [6, 8, 14, 21].

The so-called Gaussian noise (GN) model is one of the most widely-applied PLI estimates with low complexity and acceptable accuracy. Furthermore, it has been shown to have advantages when used in RSA algorithms because it is a state-dependent noise estimate and thus results in network resource saving [12, 13, 21, 22]. However, it is unable to account for demands with random bandwidth. The probabilistic spectrum Gaussian noise (PSGN) model described in [5] is a GN-model-based network-state dependent PLI estimation model that incorporates knowledge about the statistics of the traffic bandwidth. It can thus be used to estimate the accumulated noise for each demand in long-haul optical networks that use any RSA algorithm for random bandwidth traffic, including the FOOP and standard provisioning. For use in the FOOP algorithm, we must modify the PSGN model slightly to allow for spectrum overlapping.

Algorithm 3. Online Assignment Algorithm

Input: LRC demands $\mathbb{D}_{LRC}$; network topology with a set of links $\mathbb{L}$ and nodes $\mathbb{N}$; network parameters $\mathbb{F}$; Results of routed demands $\mathbb{U}_{RC}$ for $\mathbb{D}_{RC}$; Results of assigned spectrum $\mathbb{C}_{RC}$ for $\mathbb{D}_{RC}$; demand bandwidths $\mathbb{B}$.

Definitions: Same as for Algorithm 1.

procedure ONLINE ASSIGNMENT($\mathbb{D}_{LRC}$,$\mathbb{U}_{RC}$, $\mathbb{C}_{RC}$, $\mathbb{L}, \mathbb{N}, \mathbb{F}, \mathbb{B}$)

Route demands $\mathbb{D}_{LRC}$ with a desired routing algorithm:

Obtain the routing data $\mathbb{U}_{LRC}$ for $\mathbb{D}_{LRC}$

for each $q \in \mathbb{D}_{LRC}$ **do**

Based on U_q, $\mathbb{U}_{RC}$, and $\mathbb{C}_{RC}$, find the first spectrum gap starting at $f = 0$ to fit δ_q

end for

Obtain the spectrum assignment $\mathbb{C}_{LRC}$ for $\mathbb{D}_{LRC}$

end procedure

Output: $\mathbb{U}_{LRC}$ and $\mathbb{C}_{LRC}$

For deterministic bandwidth traffic, the PLI PSD per span per polarization for channel of interest q on link l is given by

$$G_{q,l} = G_{q,l}^{\text{ASE}} + G_{q,l}^{\text{NLI}}, \tag{5}$$

where $G_{q,l}^{\text{ASE}}$ and $G_{q,l}^{\text{NLI}}$ represent the PSD of ASE and NLI, respectively. The ASE noise for the channel of interest is determined only by the signal transmission distance ℓ_q. The ASE noise is usually considered the dominant PLI, but the NLI noise, which is signal dependent, still significantly impacts network resource provisioning [5,11]. We assume an ideal amplifier model for calculating the ASE noise. Therefore, the ASE noise does not depend on the demands' random bandwidths. We focus on examining the random bandwidth effects on the NLI noise, which can be large depending on the network topology and the number of demands accommodated in the networks.

The fiber nonlinearity is given by

$$G_{q,l}^{\text{NLI}} = G_{q,l}^{\text{SCI}} + G_{q,l}^{\text{XCI}} \tag{6}$$

where $G_{q,l}^{\text{SCI}}$ represents the PSD of self-channel interference (SCI) per span per polarization, and $G_{q,l}^{\text{XCI}}$ represents the PSD of the cross-channel interference (XCI) per span per polarization contributed by all channels that share the same spectrum with the channel of interest. Hence, only the nonlinear noise (the SCI and XCI) is influenced by the random bandwidths of the demands and the spectrum assignment.

The PSGN model uses the variance ($Var[\cdot]$) and expected value ($E[\cdot]$) of the SCI and the expected value of the XCI to provide a network-state dependent estimate of $G_{q,l}^{\text{NLI}}$. The PSGN PSD estimate can be written as [5]

$$G_{q,l}^{\text{PSGN}} = E[G_{q,l}^{\text{SCI}}] + r\sqrt{Var[G_{q,l}^{\text{SCI}}]} + E[G_{q,l}^{\text{XCI}}] \tag{7}$$

where r is a parameter defining how conservative the estimate is. A more conservative estimate (a larger value of r) yields a higher reliability, meaning a low risk that the actual noise exceeds the PSGN estimated noise. Empirically, the variance of the total XCI is usually more than 10 times smaller than that of SCI [5]. Therefore, we assume that the variance of XCI is negligible. Using (7), the general PLI estimate per span per polarization given in (5) can be re-written for random bandwidth traffic as

$$G_{q,l} = G_{q,l}^{\text{ASE}} + G_{q,l}^{\text{PSGN}}. \tag{8}$$

For random bandwidth demand q, $G_{q,l}^{\text{ASE}}$ can still be computed as usual [14]:

$$G_{q,l}^{\text{ASE}} = (e^{\alpha L} - 1) h\nu n_{sp}. \tag{9}$$

where L, α, n_{sp}, and ν are defined in Table 1; h is Planck's constant. $E[G_{q,l}^{\text{SCI}}]$ is calculated by [Eq. (7), 5]:

$$E[G_{q,l}^{\text{SCI}}] = \mu \mathcal{G}^3 \int_{-\infty}^{\infty} \ln(\rho\delta^2)\, dF_{\Delta_q}(\delta). \tag{10}$$

Fiber parameters are defined in Table 1. $\mu = (3\gamma^2)/(2\pi\alpha|\beta_2|)$ and $\rho = (\pi^2|\beta_2|)/2\alpha$. $\mathcal{G}$ represents the signal PSD per polarization, assumed to be the same for all channels [22]. $Var[G_{q,l}^{\text{SCI}}]$ is calculated by [Eq. (8), 5]:

$$Var[G_{q,l}^{\text{SCI}}] = \mu^2 \mathcal{G}^6 \int_{-\infty}^{\infty} \ln^2(\rho\delta^2)\, dF_{\Delta_q}(\delta) - E^2[G_{q,l}^{\text{SCI}}]. \tag{11}$$

In [Eq. (3), 5], the expected XCI, $E[G_{q,l}^{\text{XCI}}] = \sum_x E[G_{q,x,l}^{\text{XCI}}]$, where x is each demand sharing at least one link with q ($x \neq q$), must be re-written for the proposed spectrum overlapped scenario because the XCI contributed by each demand x is no longer independent. We assume that the channel of interest q is centered at frequency f_q. Using a similar idea as in [Eq. (9), 5], the expected XCI can be estimated by the Riemann sum

$$\begin{aligned} &E[G_{q,l}^{\text{XCI}}] \\ &= \mu \mathcal{G}^3 E\Big[\sum_{i=0}^{\infty} \hat{I}_{q,l}(f_q^{\text{end}}(B_q) + idf) \ln\left(\frac{|f_q^{\text{end}}(B_q) + idf - f_q| + \frac{df}{2}}{|f_q^{\text{end}}(B_q) + idf - f_q| - \frac{df}{2}} \right) \\ &+ \sum_{i=-\infty}^{0} \hat{I}_{q,l}(f_q^{\text{start}}(B_q) + idf) \ln\left(\frac{|f_q^{\text{start}}(B_q) + idf - f_q| + \frac{df}{2}}{|f_q^{\text{start}}(B_q) + idf - f_q| - \frac{df}{2}} \right) \Big] \end{aligned} \tag{12}$$

$$\begin{aligned} &= \mu \mathcal{G}^3 \Big[\sum_{i=0}^{\infty} \hat{P}_{q,l}(f_q^{\text{end}}(B_q) + idf) \ln\left(\frac{|f_q^{\text{end}}(B_q) + idf - f_q| + \frac{df}{2}}{|f_q^{\text{end}}(B_q) + idf - f_q| - \frac{df}{2}} \right) \\ &+ \sum_{i=-\infty}^{0} \hat{P}_{q,l}(f_q^{\text{start}}(B_q) + idf) \ln\left(\frac{|f_q^{\text{start}}(B_q) + idf - f_q| + \frac{df}{2}}{|f_q^{\text{start}}(B_q) + idf - f_q| - \frac{df}{2}} \right) \Big] \end{aligned} \tag{13}$$

where $f_q^{\text{end}}(B_q) = f_q^{\text{start}}(B_q) + B_q$ is the highest frequency assigned to the channel of interest q. Similarly, $f_q^{\text{start}}(B_q)$ is the lowest frequency of the channel of interest q. df is the frequency differential.

$\hat{P}_{q,l}(f)$ and $\hat{I}_{q,l}(f)$ are defined in Section 2B for evaluating the effects of channel q's adjacent channels. Equation (13) follows from (12) and (3), because the expected value in (12) applies only to $\hat{I}_{q,l}(\cdot)$. When $df \to 0$, the discrete sum becomes an integral. Eq. (13) can be simplified as in [Eq. (10)-(11), 5], and written as

$$E[G_{q,l}^{\text{XCI}}] = \mu \mathcal{G}^3 \int_{-\infty}^{f_q^{\text{start}}(B_q)} \frac{\hat{P}_{q,l}(f)}{|f - f_q|} df + \int_{f_q^{\text{end}}(B_q)}^{\infty} \frac{\hat{P}_{q,l}(f)}{|f - f_q|} df. \tag{14}$$

The detailed derivation and validation of the PSGN model for non-overlapping spectra can be found in [5]. To validate the overlapping spectrum scenario, we conducted a 1,000,000-trial Monte Carlo simulation with randomly generated traffic, the average value of the which yielded negligible error for (14) compared to the standard GN model applied to each trial [5].

The PSGN model is used in Algorithm 2 as follows. $\mathbb{G}_{RC}$, the set of PLIs, comprises the PLI estimate $G_{q,l}$ (per span per polarization) for each demand $q \in \mathbb{D}_{RC}$ and link $l \in U_q$, computed by the noise estimated in (8), where $G_{q,l}^{\text{ASE}}$ and $G_{q,l}^{\text{PSGN}}$ are given by (9) and (7), respectively. $E[G_{q,l}^{\text{SCI}}]$, $Var[G_{q,l}^{\text{SCI}}]$, and $E[G_{q,l}^{\text{XCI}}]$ are computed by (10), (11), and (14). On the network level, PLIs for each demand q accumulate over all spans of U_q during transmission.

A theory for deploying regeneration resources to negate accumulated PLIs, as step 3 in Algorithm 2, is introduced in the following section.

Table 1. System Parameters [14, 21]

Parameter	Symbol	Simulation value
Fiber power attenuation	α	0.22 dB/km
Fiber group velocity dispersion	β_2	$-21.7\,\text{ps}^2/\text{km}$
Fiber nonlinearity	γ	$1.32 \times 10^{-3}\,(\text{W}\cdot\text{m})^{-1}$
Light frequency	ν	193.55 THz
Spontaneous emission factor	n_{sp}	1.58
Fiber length per span	L	100 km

4. REGENERATION NODES DEPLOYMENT FOR RANDOM BANDWIDTH TRAFFIC

As discussed above, during signal transmission through long-haul optical backbone networks, the accumulated noise severely impairs the QoT. The transmitted data cannot be appropriately decoded if the accumulated noise exceeds the required noise threshold. Regeneration nodes are used to refresh the signal and fully negate the accumulated noise by performing an optical-electrical-optical (OEO) process of re-timing, re-shaping, and re-amplification [6]. However, regeneration nodes are scarce resources due to the high cost of the requisite equipment and its maintenance. Thus, regeneration nodes must be carefully planned and deployed. A regeneration node contains regeneration circuits, and each regeneration circuit serves one light-path. Considering the limited number of transceivers per reconfigurable optical add-drop multiplexer (ROADM) [1] and data processing ability per regeneration node [23], the number of circuits per regeneration node is limited.

In this section, we use a path-based MILP algorithm to optimize the assignment of regeneration resources to nodes. The network is modeled as a connected graph $(\mathbb{N}, \mathbb{L})$. Note, for a better description of the MILP formulation, we refine the notation of the unidirectional link l as $l_{i,j}$, representing the source node

i and destination j for the signal propagation direction. $\mathbb{D}_{RC}$ is the demands set used by the MILP algorithm. The optimization objective is $\varepsilon T + C$, where T is the total number of regeneration nodes needed; C is the total number of regeneration circuits used; and ε is a balancing factor.

The PSGN model (8) provides a link-based noise estimation $G_{q,l}$ for each demand per span per polarization. $\hat{G}_{q,l_{i,j}}$ represents the link level PSGN estimated noise for demand $q \in \mathbb{D}_{RC}$ on link $l_{i,j}$, $\hat{G}_{q,l_{i,j}} = G_{q,l=l_{i,j}} \|l_{i,j}\|$, where $\|l_{i,j}\|$ is the number of spans on link $l_{i,j}$. $Z_{q,n} \in \mathbb{R}$ represents the accumulated noise at node n for demand q. $\mathcal{I}_n$ is a binary variable used as a regeneration node indicator: if node n is a regeneration node, $\mathcal{I}_n = 1$; otherwise, $\mathcal{I}_n = 0$. $\mathcal{I}_{q,n}$ is a binary decision variable indicating if a regeneration circuit is assigned at node n for demand q, ($\mathcal{I}_{q,n} = 1$), and otherwise, $\mathcal{I}_{q,n} = 0$. Suppose that the route U_q consists of consecutive nodes $n_1, n_2, \ldots, n_M$. Then Z_{q,n_i} at node n_i, for $i = 1, \ldots, M$, is given by

$$Z_{q,n_i} = \begin{cases} 0, & \text{if } i = 1 \text{ or } \mathcal{I}_{q,n_i} = 1, \\ Z_{q,n_{i-1}} + \hat{G}_{q,l_{n_{i-1},n_i}}, & \text{otherwise,} \end{cases} \tag{15}$$

which represents the noise accumulation along the route from the beginning node of the transparent segment (light-path without regeneration) to node n_i.

The constraint enforcing that regeneration circuits can only be applied at regeneration nodes is given by

$$\sum_{q \in \mathbb{D}_{RC}} \mathcal{I}_{q,n} \leq \mathcal{I}_n \mathcal{I}^{\max}, \qquad \forall n \in \mathbb{N}, \tag{16}$$

where $\mathcal{I}^{\max}$ is the maximum number of circuits per regeneration node. The objective function variables are accumulated using

$$T = \sum_{n \in \mathbb{N}} \mathcal{I}_n; \tag{17}$$

$$C = \sum_{n \in \mathbb{N}, q \in \mathbb{D}_{RC}} \mathcal{I}_{q,n}; \tag{18}$$

which count the total number of regeneration nodes and regeneration circuits used, respectively.

The ratio of input signal power $\mathcal{G}$ to accumulated noise for each demand q is given by

$$\frac{\mathcal{G}}{Z_{q,n_i}} \geq \text{SINR}_{th}, \qquad \forall q \in \mathbb{D}_{RC}, n \in \mathbb{N}, \tag{19}$$

which should always be greater than the required signal to interference plus noise ratio (SINR) threshold SINR_{th} for demand q in order to satisfy the QoT requirements.

5. SIMULATION SETTINGS AND NUMERICAL RESULTS

In order to test the performance of the proposed algorithm, numerous network-level simulations were conducted. The following simulation results demonstrate the benefits of using the proposed FOOP algorithm and the PSGN model.

A. Traffic Model

We simulated realistic traffic in a real continental-scale network to show the potential benefits to industry brought by the proposed algorithm. The traffic model used is based on statistics from [24]: the average demand bandwidth is related to the traffic volume, which is estimated based on the population served by pairwise network nodes, provided by [24], and the bandwidth variance is a function of the traffic variance, which is estimated based on the statistics from major operators [4]. In accordance with [4], we categorize each traffic demand bandwidth using three realizations: large, medium, and small, which are representative of the traffic volume experienced in one day (corresponding to rush hour traffic δ_L, normal traffic δ_M, and light traffic δ_S scenarios) with bandwidth realization probabilities $\Pr(\Delta = \delta_L) = 5/24$, $\Pr(\Delta = \delta_M) = 12/24$, and $\Pr(\Delta = \delta_S) = 7/24$. In simulation, the same random bandwidth traffic is applied to all algorithms in all scenarios. The time-varying demand bandwidths are considered as statistically independent in Sections 5C and 5D. Correlated traffic is simulated in Section 5E.

B. Simulation Settings

The NSF-24 network with $|\mathbb{N}| = 24$ nodes and $|\mathbb{L}| = 86$ links is used to test the proposed algorithm. We assume a flexible grid network with spectrum slices of 6.25 GHz, with 4400 GHz of available spectrum (C-band). We consider that each node in the network communicates with all the others, i.e., the total number of demands is $|\mathbb{N}| \times (|\mathbb{N}| - 1) = 552$. All demands use the same modulation format. Neither wavelength conversion nor modulation conversion is utilized. The simulation parameters are listed in Table 1.

C. Network Planning: Spectrum Usage, Network Throughput, and Transmission Loss

In this section, we test the proposed FOOP algorithm to establish a trade-off between spectrum usage, network throughput, and transmission loss. The spectrum usage reflects the provisioning efficiency of the proposed algorithm.

The network throughput is a metric to show the transmission capacity of the algorithm. The average network throughput is the data from the accommodated demands minus the transmission loss caused by the rare occurrence of spectrum collisions, calculated as

$$\text{Average throughput} = \eta \sum_q \int_{-\infty}^{\infty} S_{q,l}(f) df - \text{Transmission Loss}, \tag{20}$$

where η is the modulation spectral efficiency, and the sum is over all demands.

The transmission loss measures the stability of the proposed algorithm. In this section, we consider the occurrence of any assigned-spectrum overlap as causing data loss, as a worst-case scenario. The transmission loss and, consequently, the network throughput, are calculated using a path-based approach, i.e., they are calculated along the light-path from the source to the destination. The transmission loss can be derived using

$$\text{Transmission Loss} = \eta \sum_q \int_{f_q^{\text{start}}(B_q)}^{f_q^{\text{end}}(B_q)} 1 - \prod_{l \in U_q} [1 - P_l^{\text{OL}}(f)] df. \tag{21}$$

It is thus calculated by considering the probability of the data lost by spectrum overlapping $P_l^{\text{OL}}(f)$, accumulated along the demand route U_q over all demands.

Two benchmark algorithms are used for comparison: standard provisioning (static provisioning according to the maximum bandwidth for each demand, equivalent to the FOOP with $B = 0\%$) and median provisioning (static provisioning that uses the median value of the bandwidth for each demand, independent of B; in our simulation settings, the median value of a random bandwidth equals the value of its medium-sized bandwidth realization δ_M). For fairness in comparison, the benchmark algorithms also comprise an offline static provisioning

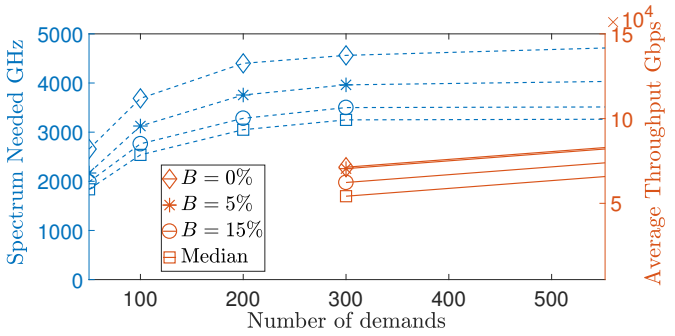

Fig. 2. Spectrum usage and average network throughput versus number of demands provisioned in the network for the Hybrid demand ordering scheme.

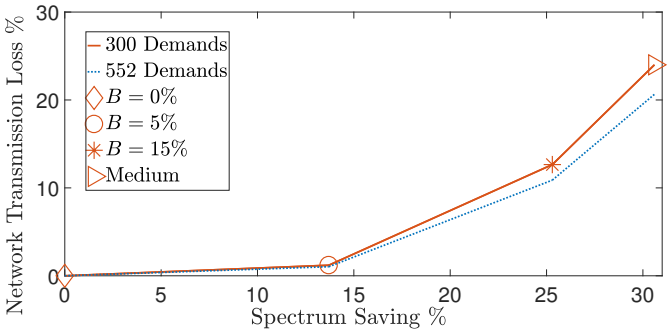

Fig. 3. Network transmission loss versus spectrum savings for demands $\mathbb{D}_{RC}$ and $\mathbb{D}$ provisioned using the Hybrid scheme.

step and an online dynamic portion. For the offline part, the benchmarks execute resource provisioning without considering any randomness in the demand bandwidth. The online part of the benchmark algorithms is similar to the proposed FOOP algorithm.

Further simulation details are as follows. Two overlapping probability thresholds, $B = 5\%$ and 15%, are simulated. In this section, the modulation format used for all demands is polarization-multiplexed quadrature phase-shift keying (PM-QPSK), requiring a pre-forward-error-correction (pre-FEC) bit error rate (BER) of 4×10^{-3} ($\text{SINR}_{th} = 8.47$ dB) [8, 14, 25]. To balance hardware pressures and algorithm scalability, the number of demands processed in the offline static provisioning, $|\mathbb{D}_{RC}|$, using Algorithm 2 is 300 (RC demands) and the remaining $|\mathbb{D}_{LRC}| = 252$ LRC demands are accommodated by the online Algorithm 3.

We also consider different RC demand selection based on the demand ordering scheme H. We test three schemes H, showing three representative cases: considering bandwidth only ($\varpi = 0$), denoted as *BW*, routing only ($\chi = 0$), denoted as *Hops*, and a hybrid of bandwidth and routing ($\varpi/\chi = 1/20\,\text{GHz/km}$), which makes $\varpi\ell_q$ and $\chi \max \Delta_q$ comparable, denoted as *Hybrid*. The simulation results of different demand ordering schemes result in different performances but a similar trend. For illustration purposes, in this section we present results based on the Hybrid demand ordering scheme.

Figure 2 shows both the spectrum needed by the provisioning algorithms (on the left-side axis) and the network throughput (on the right-side axis) versus the number of demands accommodated. The first 50 demands require almost as much spectrum as that needed by the remaining 502 demands. Furthermore, with the resource-consuming demands $\mathbb{D}_{RC}$ provisioned, the remaining LRC demands $\mathbb{D}_{LRC}$ require few additional spectrum resources.

Figure 2 quantifies the trade-off between resource savings (spectrum needed) and capacity (network throughput). Standard provisioning has the highest throughput but requires significantly more spectrum than the 4400 GHz provided by C-band [1]. The FOOP algorithm with $B = 5\%$ has almost the same throughput compared to standard provisioning, yet saves 14% of the spectrum needed. Median provisioning and FOOP with $B = 15\%$ require a decrease of 31% and 25% in spectrum required, respectively, compared to standard provisioning, which is much less than that needed by FOOP with $B = 5\%$. But these provisioning algorithms sacrifice too much data throughput (on the order of 10^5 Gbps throughput loss). Therefore, median provisioning and FOOP with $B = 15\%$ are not sufficiently robust to employ in backbone networks, and we do not discuss these further.

The intentionally designed spectrum overlap between neighboring channels saves spectrum resources but potentially results in transmission loss, as shown in Figure 3. Considering only the 300 RC demands, $\mathbb{D}_{RC}$, standard provisioning ($B = 0\%$) has no transmission loss since it reserves the maximal resources needed by demands. The FOOP algorithm with $B = 5\%$ results in less than 2% data transmission loss, which is negligible, but saves 14% of spectrum resources. Median provisioning is independent of the overlapping probability threshold B; it results in 25% data loss. The LRC demands $\mathbb{D}_{LRC}$ induce zero transmission loss since they are provisioned with the online algorithm based on their maximum bandwidth needs. For the other demand sorting schemes H (BW and Hops), the trends in the results are similar to the Hybrid; the performance of these schemes is described in the next section.

In summary, saving on the required spectrum is achieved at the cost of a potential loss of data transmission in the network. However, the selection of a small overlapping probability threshold of $B = 5\%$ leads to a negligible throughput loss with a substantial spectrum saved. For all subsequent analyses, we use $B = 5\%$ when referring to the FOOP algorithm.

To test the robustness of the FOOP algorithm to uncertainties in the traffic bandwidth distribution, two scenarios were simulated assuming an inaccurate traffic CDF. We consider the CDF of the demands in Section 5A as the benchmark. We first simulate a worst-case scenario where the FOOP is based on the benchmark CDF, but the actual demand bandwidths are their maximum values. (All other simulation settings remain unchanged.) The transmission loss for this scenario is severe, 26%. Second, we simulate the scenario with a less extreme mismatched CDF estimate: the FOOP is based on the benchmark CDF, but the actual demand bandwidths are normally distributed with the same mean and variance as the benchmark. The transmission loss for this scenario is 8%, which is still significantly higher than the 2% transmission loss observed when the CDF is known precisely. Therefore, obtaining an accurate demand CDF is essential for our probabilistic resource provisioning algorithm. However, with the current emphasis on network monitoring, we expect that the characteristics of the heterogeneous traffic will be well understood in the near future.

D. Network Operation: Bottleneck Demand Selection

Network resource usage depends significantly on the sequence of demands accommodated [3, 14, 20]. In this section, we ana-

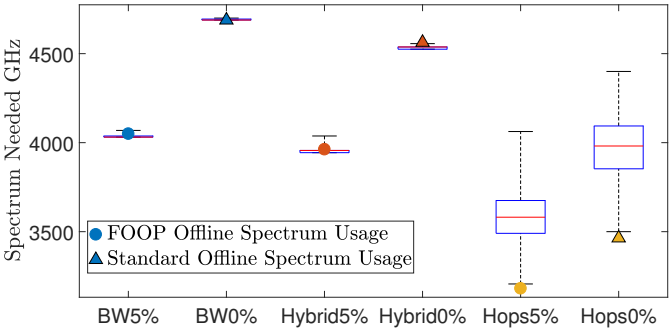

Fig. 4. Simulated distribution of the total spectrum usage for three resource consumption orderings. The solid dots and triangles are the offline provisioning results for demands in $\mathbb{D}_{RC}$ for the FOOP ($B = 5\%$) and standard provisioning ($B = 0\%$), respectively. The box plot shows the maximum, upper quartile, median, lower quartile, and the minimum.

lyze the impact of the ordering scheme, H, on network resource usage. The criteria named above Hybrid, BW, and Hops are investigated. We simulate the FOOP and the benchmark algorithm, standard provisioning, using a 100,000 trial Monte Carlo simulation. The Monte Carlo simulation randomly selects the bandwidth of demands in $\mathbb{D}$ according to their probabilities in order to test the operational performance given the pre-planned results. The operational spectrum usage for demands $\mathbb{D}_{RC}$ with randomly selected bandwidth is unvarying since it is pre-planned with probabilistic information. However, the spectrum usage for $\mathbb{D}$ will vary because $\mathbb{D}_{LRC}$ with randomly selected bandwidth can fill the spectrum fragmentation using the online provisioning scheme. The network transmission loss and the average throughput are also verified in this section by the Monte Carlo simulation, where the analytic results in Sections 5 C are shown to be consistent with the results of the simulation.

Figure 4 shows the distributions of spectrum usage for the three different criteria obtained by Monte Carlo simulation for the FOOP and standard provisioning. When all demands $\mathbb{D}$ are provisioned, the spectrum usage of the FOOP algorithm is again significantly lower than that of the standard provisioning, consistent with the pre-planning results in Section 5 C. The Hops scheme has the lowest static spectrum needed for provisioning demands in $\mathbb{D}_{RC}$, with the actual spectrum usage for all demands $\mathbb{D}$ constantly and significantly exceeding the pre-planned resources for the RC demands. This is because static provisioning for the Hops criterion only accommodates demands with long routes, and some of the remaining demands have large bandwidths. These remaining demands in $\mathbb{D}_{LRC}$ cannot fit into the spectrum gaps left by provisioning the longest-route demands $\mathbb{D}_{RC}$, which results in a need for additional spectrum. Thus the Hops scheme leads to tremendous disruption during the online stage; it results in excessive hardware pressure and immoderate burden on the control plane.

For the FOOP algorithm, the Hybrid scheme requires 3% less spectrum for static provisioning of the resource-consuming demands than the BW scheme. In most cases, shown by the box-plot in Figure 4, the subsequent dynamic provisioning does not require additional spectrum resources beyond the static provisioning, which leads to infrequent disruption. The spectrum reserved by the static provisioning step for both the BW and Hybrid schemes usually suffices for all demands in $\mathbb{D}$, but the Hybrid scheme saves more spectrum than the BW method. In addition, the design margin between the maximum spectrum (top of the box plot) and the static result (solid dot) for the Hybrid is larger than that of the BW for the FOOP algorithm. This means that given a smart operational scheme, the Hybrid scheme would have more flexibility than the BW scheme. Lastly, considering the factors impacting the PLIs (bandwidth and accumulated length) [8], the Hybrid scheme is more comprehensive for regeneration resource deployment, which does not consider the LRC demands. In summary, as shown in Figure 4, the Hybrid scheme provides the best trade-off among the three ordering criteria because its static provisioning efficiently reserves spectrum for the RC demands, mitigates the disruption caused by dynamic provisioning, and aligns with the nature of the PLIs.

E. Correlated Traffic

The scenarios in Sections 5 C and D assume that the demand bandwidths are statistically independent of each other, i.e., the probability of demand bandwidths varies independently. However, realistic traffic in optical backbone networks is often correlated and varies with time. For example, a higher traffic volume between all pairs of nodes is expected at major sports and entertainment events. The assumption of uncorrelated traffic volume may not yield results that are representative of correlated traffic. Therefore, we simulate a scenario where the traffic volume between adjacent demands sharing a link is correlated. The conditional probability that a channel x adjacent to the channel of interest q on a link has a large bandwidth, given that q has a large bandwidth, is denoted by P_{corr}. For the previous discussion assuming independent traffic, based on the probability of large, medium, and small bandwidth traffic, $P_{\text{corr}} = 7/24$. We simulate three additional cases: $P_{\text{corr}} = 1$, where the traffic is totally correlated, $P_{\text{corr}} = 0.5$, and $P_{\text{corr}} = 0.7$.

In general, a varying P_{corr} will not result in a fixed overlap probability threshold B. For example, the threshold $B = 5\%$ is too strict to yield a high P_{corr}. A higher value of B will result in an unacceptable transmission loss in the low P_{corr} case. For the results in this section, the network transmission loss is fixed at 2% (equal to the network transmission loss with independent traffic and $B = 5\%$ in Figure 2). We adopt a similar spectrum overlapping situation as in the uncorrelated $B = 5\%$ case, where overlapping occurs only when two adjacent channels x and q both have a large bandwidth, i.e., $\Delta_q = \delta_L$ and $\Delta_x = \delta_L$. The spectrum assignment $S_{q,l}(f)$ can be obtained by using (20) and (21), where the network transmission loss is fixed at 2%, and $P_l^{\text{OL}}(f)$ from (2) in this scenario can be re-written as

$$\begin{aligned} P_l^{\text{OL}}(f) &= \Pr[\sum_q I_{q,l}(f) > 1] \\ &= \Pr[\Delta_x = \delta_L, \Delta_q = \delta_L] = \Pr[\Delta_q = \delta_L] P_{\text{corr}}, \end{aligned} \tag{22}$$

where $\Pr[\Delta_x = \delta_L, \Delta_q = \delta_L]$ is the joint probability that two adjacent channels (x and q) have large bandwidth, and $\Pr[\Delta_q = \delta_L]$ is the probability that the channel of interest q has a large bandwidth.

Except for the conditional probability of the bandwidth in adjacent channels, all simulation settings remain the same as above. Only the offline provisioning phase in the FOOP algorithm is simulated since the bandwidths of demands in the online provisioning phase are taken as deterministic. The offline provisioning is executed by replacing the constraint $P_l^{\text{OL}}(f) \leq B, \forall f$ in step 1 of Algorithm 2 with the modified constraint (22).

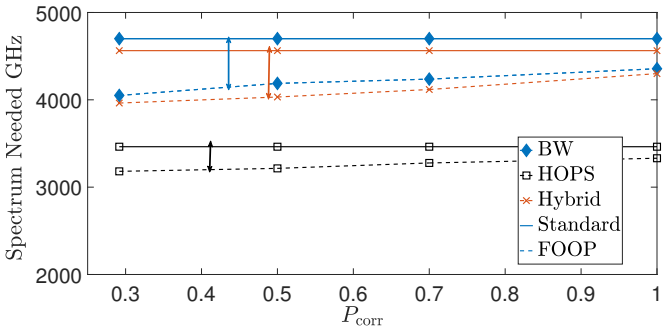

Fig. 5. Spectrum needed as a function of P_{corr} for three demand ordering schemes.

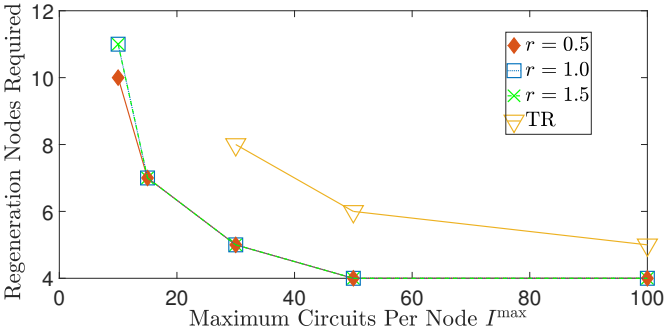

Fig. 6. Number of regeneration nodes required as functions of the maximum number of regeneration circuits per node, $\mathcal{I}^{max}$, with the FOOP algorithm using the PSGN model with various r and the TR model; PM-QPSK modulation.

Figure 5 shows the effect that different bandwidth correlation levels have on the required spectrum. For the FOOP algorithm, an increase in the correlation results in an increase in the spectrum needed. For the Hybrid demand ordering scheme, the independent traffic scenario requires 9% less spectrum than the totally correlated traffic. The spectrum required for practical traffic, where the correlation may vary with time, should remain around the dashed lines. The double arrows show the spectrum saving brought by the FOOP for correlated bandwidth demands compared to standard provisioning. The spectrum needed using standard provisioning does not depend on P_{corr}. The FOOP algorithm saves spectrum, even for highly correlated demands. The spectrum saving brought by the FOOP algorithm varies from 6% to 14% for the Hybrid demand ordering scheme.

F. Regeneration Resource Deployment

For long-haul optical networks such as the NSF-24 network, regeneration resources are required to maintain error-free data transmission. OEO processing ability and the parameters of the ROADMs at the regeneration nodes limit the number of regeneration circuits per node [6, 23, 26, 27]. Regeneration nodes and circuits are scarce resources and need to be efficiently deployed. Regeneration resources are static resources and have to be preplanned by an offline method. In this section, we use the results of Steps 1 and 2 of the offline Algorithm 2 in the regeneration resource assignment. For the reasons given in Section 5D, we use the Hybrid demand ordering scheme for the results in this section.

In order to efficiently deploy the regeneration resources, accurate PLI estimates are necessary. In this section, we optimize the regeneration resource deployment using the proposed PSGN model and compare it with the widely-applied TR model as a benchmark.

F.1. Regeneration for PM-QPSK Modulation

We simulate the regeneration resource deployment algorithm, described in Section 4, on the NSF-24 network using PM-QPSK modulation with both the PSGN and TR models. The TR model is the most conservative model considering the worst-case transmission reach for the maximum bandwidth of the random bandwidth demands. We compare the number of regeneration nodes and circuits needed for both standard provisioning and the FOOP algorithm for the same demands, assuming that the demand bandwidths are statistically independent.

Figure 6 shows results on the number of regeneration nodes needed with a different maximum number of circuits per node, $\mathcal{I}^{max}$, for the FOOP algorithm. The factor r is a measure of how

Table 2. Regeneration nodes and circuits required using the PSGN model for PM-QPSK modulation

			Regeneration Nodes		
		Circuits	$\mathcal{I}^{max}=10$	$\mathcal{I}^{max}=15$	$\mathcal{I}^{max}=30$
$B=5\%$	$r=0.5$	95	10	7	5
	$r=1.0$	99	11	7	5
	$r=1.5$	101	11	7	5
	TR	188	N/A	N/A	8
$B=0\%$	$r=0.5$	88	9	7	5
	$r=1.0$	90	9	7	5
	$r=1.5$	95	10	7	5
	TR	188	N/A	N/A	8

conservative is the PSGN model, as described in Section 3. For $\mathcal{I}^{max}$ less than 50, the number of regeneration nodes required decreases steeply as $\mathcal{I}^{max}$ increases. The algorithm using the PSGN model has a looser $\mathcal{I}^{max}$ requirement compared to the TR model. With $\mathcal{I}^{max} = 10$ or 15, the algorithm using the TR model has no solution for the NSF-24 network. Therefore, network operators using the TR model require more advanced ROADMs and higher data processing abilities.

As shown in Table 2, for $\mathcal{I}^{max} = 30$, the PSGN model requires 37.5% fewer regeneration nodes and less than half of the regeneration circuits than the TR model. For $\mathcal{I}^{max} = 10$, using the smallest r, $r = 0.5$, saves 10% and 6% of the regeneration nodes and circuits required, respectively, compared to using a higher r, $r = 1.5$. The additional six regeneration circuits needed with $r = 1.5$ implies that there are six demands that might fall short of the required SINR threshold compared to less conservative planning, i.e., $r = 0.5$. This shows a trade-off between network resources and planning robustness: a more conservative PLI estimate leads to an increase in regeneration resources needed. In general, the small loss in robustness can be absorbed by normal network margins. For algorithms using the TR model, more than half of the demands require regeneration at intermediate nodes of the routes during transmission, as shown in Table 2. This wastes tremendous network resources for OEO processing, including hardware resources, computational resources, and power, in order to gain the ultimate robustness in transmission.

For the standard provisioning algorithm ($B = 0$), spectrum

Table 3. Two higher-order modulation formats applicable to the NSF-24 network

Modulation format	PM-QPSK	PM-8QAM
SINR_{th}	8.47 dB	10.8 dB
pre-FEC BER	4×10^{-3}	2.2×10^{-2}
FEC code	Staircase code OH 6.25%	Staircase code OH 33.3%
Net spectral efficiency	3.8 bit/symbol	4.5 bit/symbol

is reserved for the maximum bandwidth needs of the demands, but the demands' bandwidths are still random and time-varying. The spectrum assigned to neighboring channels does not overlap. For standard provisioning, also shown in Table 2, the PSGN model again shows significant savings on regeneration nodes and circuits compared to the TR model, of 38% and 49%, respectively, for $\mathcal{I}^{\max} = 30$.

For systems that use smaller ROADMs with $\mathcal{I}^{\max} = 10$, the FOOP algorithm requires 11% more regeneration nodes and 8% more regeneration circuits, respectively, compared to standard provisioning ($B = 0$). Standard provisioning has lower PLIs than the FOOP algorithm because the XCI for $B = 5\%$ is higher than for $B = 0\%$; the SCI of the random bandwidth demands is the same for both algorithms since it is independent of B. The higher XCI of $B = 5\%$ is the result of a more compact spectrum assignment than that of $B = 0\%$, i.e., we intentionally overlap the spectrum allocation in order to save spectrum. Therefore, we conclude that increasing B results in an increase in the PLIs, and thus leads to the need for more regeneration resources.

F.2. Regeneration for Higher-Order Modulation Formats

High order modulation formats are desired to solve the spectrum shortage problem by increasing the spectral efficiency. In the near future, saving spectrum by applying higher-order modulation formats is a potential solution for the rapid increase in data volume expected. However, higher-order modulation formats require a higher SINR threshold in order to maintain error-free data recovery, i.e., a negligible post-FEC BER of 10^{-15} [28]. The stricter SINR threshold leads to a need for more regeneration resources. In this section, we simulate the NSF-24 network and estimate the regeneration resources needed when a higher-order modulation format is applied. We do not consider modulation conversion and maintain the same modulation format for all demands due to the current high costs of implementing this technology. When we choose a modulation, we vary the data-rate and not the bandwidth so that, as the order of the modulation format increases, the total network throughput increases.

We vary the SINR threshold in the MILP algorithm used to assign regeneration nodes and circuits. The combination of the SINR threshold and the modulation format determines the pre-FEC BER and, therefore, which FEC code is needed to maintain error-free transmission. The lowest SINR_{th} considered is 8.47 dB, suitable for PM-QPSK modulation [8, 14, 25] with a pre-FEC BER of 4×10^{-3}, which can be corrected down to a post-FEC BER of 10^{-15} using a staircase code with overhead (OH) of 6.25% [29]. On the high end, we push the system up to an $\text{SINR}_{th} = 10.8$ dB, which suffices for PM-8QAM (8-ary quadrature amplitude modulation) to achieve a pre-FEC BER of 2.2×10^{-2} [28, 30], requiring a staircase code with 33.33% OH to achieve the same post-FEC BER [29]. Comparing PM-QPSK with a 6.25% OH code and PM-8QAM with a 33.33% OH code, the net spectral efficiency is increased from $4/(1 + 0.0625) = 3.8$ bits/symbol to $6/(1 + 0.3333) = 4.5$ bits/symbol, an increase of 18%. These parameters are summarized in Table 3. Note that PM-8QAM with an $\text{SINR}_{th} \geq 11$ dB does not work because the required SINR is too high for the continental-scale NSF-24 network: some links are too long, and thus the signal accumulates too much noise given the input signal PSD.

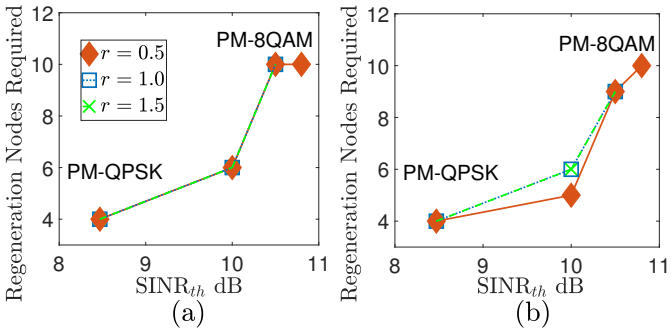

Fig. 7. Regeneration nodes needed versus SINR_{th}. (a) $\mathcal{I}^{\max} = 50$ (b) $\mathcal{I}^{\max} = 100$.

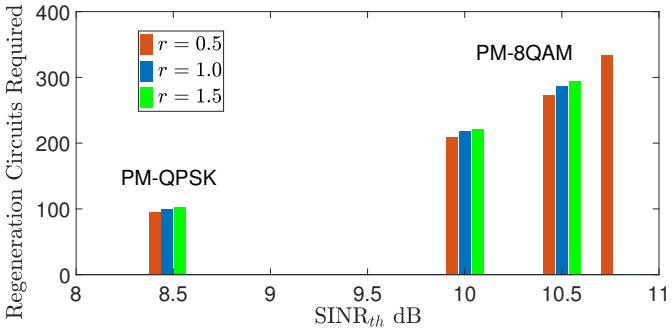

Fig. 8. Regeneration circuits needed for various SINR thresholds, estimated using the PSGN model with various r; $\mathcal{I}^{\max} = 50$.

Figure 7 shows the number of regeneration nodes needed for various SINR_{th} for $I\mathcal{I}^{\max} = 50$ and $\mathcal{I}^{\max} = 100$. The network is able to operate at an $\text{SINR}_{th} = 10.8$ dB (suitable for PM-8QAM) using the PSGN with $r = 0.5$, but $r = 1.0$ and $r = 1.5$ are too strict for error-free transmission. $\mathcal{I}^{\max} = 100$ requires up to 16% fewer regeneration nodes than $\mathcal{I}^{\max} = 50$. PM-8QAM cannot be deployed by using the TR model with any value of $\mathcal{I}^{\max}$ because of the long links; the PLIs predicted by the TR model lead to an SINR estimate that is below the required SINR threshold. Thus, networks using the PSGN model can use PM-8QAM to achieve 18% higher net spectral efficiency compared to networks using the TR model, which can only function with PM-QPSK. In our results, intermediate values of the SINR_{th} of 10 and 10.5 dB are included only for completeness and not matched with any particular modulation scheme and code.

Figure 8 shows how many regeneration circuits are needed for the various SINR_{th}, using the PSGN model with various r. Choosing $r = 0.5$ saves up to 8% of the regeneration circuits at an $\text{SINR}_{th} = 10.5$ dB compared to choosing $r = 1.5$. For an $\text{SINR}_{th} = 10.8$ dB, the network requires 337 regeneration circuits, which means that most of the demands need to be refreshed at least once in order to negate the noise and keep the signal SINR high enough for transmission. A network that provides an $\text{SINR}_{th} = 10.8$ dB can increase the spectral efficiency by 18% compared to $\text{SINR}_{th} = 8.47$ dB at the cost of 150% more

regeneration nodes and 251% more regeneration circuits. The number of regeneration circuits with these high-order modulation formats needs to be high because the PLIs are worse. With the development of ROADMs equipped with more circuits and more advanced OEO processing techniques, the benefits of using higher spectral efficiency modulation will be an appealing solution to address the constantly increasing data volume.

In brief, there is a trade-off between spectral efficiency, regeneration resources, and reliability. Reliability and spectral efficiency increase at the cost of an increase in regeneration resources needed. With fixed regeneration resources, reliability decreases with increasing spectral efficiency. The most spectrally-efficient solution for the NSF-24 network is to use PM-8QAM with the FOOP algorithm based on the PSGN model—the TR model is too conservative to allow higher order modulations to be used.

6. CONCLUSIONS

In this paper, we propose an algorithm called the FOOP for resource provisioning of random bandwidth demands. The FOOP algorithm comprises a static offline planning phase for resource-consuming demands and a dynamic online phase to accommodate low-resource-consuming demands. This two-step process balances provisioning performance, hardware pressure, and network flexibility. We use the newly proposed PSGN model, which can be designed to be more or less conservative based on operator needs, for estimating the PLI of random bandwidth demands. The PSGN model is also suitable for aggressive spectrum allocation scenarios. The FOOP algorithm with $B = 5\%$ saves 14% of the spectrum resources with less than 2% throughput loss. Compared to the widely applied TR model, utilizing the PSGN model has a remarkable savings of 49% in the regeneration resources needed. In addition, with the appropriate modulation formats, sufficient regeneration resources, and appropriate FEC codes, the PSGN model enables the whole networks to operate at an 18% higher net spectral efficiency than the TR model.

7. ACKNOWLEDGMENT

This work was supported in part by NSF grant CNS-1718130.

REFERENCES

1. O. Gerstel, M. Jinno, A. Lord, and S. Yoo, "Elastic optical networking: A new dawn for the optical layer?" IEEE Commun. Mag. **50**, 12–20 (2012).
2. K. Christodoulopoulos, I. Tomkos, and E. Varvarigos, "Elastic bandwidth allocation in flexible OFDM-based optical networks," IEEE J. Light. Technol. **29**, 1354–1366 (2011).
3. B. C. Chatterjee, N. Sarma, and E. Oki, "Routing and spectrum allocation in elastic optical networks: A tutorial," IEEE Commun. Surv. Tuts. **17**, 1776–1800 (2015).
4. M. Feknous, T. Houdoin, B. L. Guyader, J. D. Biasio, A. Gravey, and J. A. T. Gijón, "Internet traffic analysis: A case study from two major European operators," in *IEEE Symp. Comput. Commun. (ISCC),* (2014).
5. Y. Xu, E. Agrell, and M. Brandt-Pearce, "Probabilistic spectrum Gaussian noise estimate for random bandwidth traffic," in *Proc. European Conference on Optical Communication (ECOC),* (2019).
6. X. Wang, M. Brandt-Pearce, and S. Subramaniam, "Impact of wavelength and modulation conversion on translucent elastic optical networks using MILP," J. Opt. Commun. Netw. pp. 644–655 (2015).
7. I. Tomkos, S. Azodolmolky, J. Solé-Pareta, D. Careglio, and E. Palkopoulou, "A tutorial on the flexible optical networking paradigm: State of the art, trends, and research challenges," Proc. IEEE **102**, 1317–1337 (2014).
8. L. Yan, Y. Xu, M. Brandt-Pearce, N. Dharmaweera, and E. Agrell, "Robust regenerator allocation in nonlinear flexible-grid optical networks with time-varying data rates," J. Opt. Commun. Netw. pp. 823–831 (2018).
9. M. Cantono, R. Gaudino, and V. Curri, "Potentialities and criticalities of flexible-rate transponders in DWDM networks: A statistical approach," J. Opt. Commun. Netw. pp. A76–A85 (2016).
10. M. Klinkowski, M. Ruiz, L. Velasco, D. Careglio, V. Lopez, and J. Comellas, "Elastic spectrum allocation for time-varying traffic in flexgrid optical networks," J. Sel. Areas Commun. **31**, 26–38 (2013).
11. Y. Xu, E. Agrell, and M. Brandt-Pearce, "Static resource allocation for dynamic traffic," in *Proc. European Conference on Optical Communication (ECOC),* (2019).
12. P. Poggiolini, G. Bosco, A. Carena, V. Curri, Y. Jiang, and F. Forghieri, "The GN-model of fiber non-linear propagation and its applications," J. Light. Technol. **32**, 694–721 (2014).
13. P. Johannisson and E. Agrell, "Modeling of nonlinear signal distortion in fiber-optic networks," J. Light. Technol. **32**, 4544–4552 (2014).
14. Y. Xu, L. Yan, E. Agrell, and M. Brandt-Pearce, "Iterative resource allocation algorithm for EONs based on a linearized GN model," IEEE/OSA J. Opt. Commun. Netw. **11**, 39–51 (2019).
15. C. Delezoide, K. Christodoulopoulos, A. Kretsis, N. Argyris, G. Kanakis, A. Sgambelluri, N. Sambo, P. Giardina, G. Bernini, D. Roccato, A. Percelsi, R. Morro, H. Avramopoulos, E. Varvarigos, P. Castoldi, P. Layec, and S. Bigo, "Marginless operation of optical networks," J. Light. Technol. **37**, 1698–1705 (2019).
16. Y. Pointurier, "Design of low-margin optical networks," IEEE/OSA J. Opt. Commun. Netw. **9**, A9–A17 (2017).
17. A. S. Thyagaturu, A. Mercian, M. P. McGarry, M. Reisslein, and W. Kellerer, "Software Defined Optical Networks (SDONs): A Comprehensive Survey," IEEE Commun. Surv. Tutorials **18**, 2738–2786 (2016).
18. R. Dutta and G. N. Rouskas, "Traffic grooming in WDM networks: past and future," IEEE Netw. **16**, 46–56 (2002).
19. T. Zami, I. F. de Jauregui Ruiz, A. Ghazisaeidi, and B. Lavigne, "Growing impact of optical filtering in future WDM networks," in *Proc. Optical Fiber Communication Conference (OFC),* (2019).
20. M. Klinkowski and K. Walkowiak, "Routing and spectrum assignment in spectrum sliced elastic optical path network," IEEE Commun. Lett. **15**, 884–886 (2011).
21. L. Yan, E. Agrell, H. Wymeersch, and M. Brandt-Pearce, "Resource allocation for flexible-grid optical networks with nonlinear channel model," J. Opt. Commun. Netw **7**, B101–B108 (2015).
22. J. Zhao, H. Wymeersch, and E. Agrell, "Nonlinear impairment-aware static resource allocation in elastic optical networks," J. Light. Technol. **33**, 4554–4564 (2015).
23. W. Lautenschlaeger, N. Benzaoui, F. Buchali, L. Dembeck, R. Dischler, B. Franz, U. Gebhard, J. Milbrandt, Y. Pointurier, D. Roesener, L. Schmalen, and A. Leven, "Optical Ethernet—flexible optical metro networks," J. Light. Technol. **35**, 2346–2357 (2017).
24. M. Batayneh, D. A. Schupke, M. Hoffmann, A. Kirstaedter, and B. Mukherjee, "On routing and transmission-range determination of multi-bit-rate signals over mixed-line-rate WDM optical networks for carrier ethernet," IEEE/ACM Trans. Netw. **19**, 1304–1316 (2011).
25. D. J. Ives and S. J. Savory, "Transmitter optimized optical networks," in *Opt. Fiber Commun. Conf. Exhib. (OFC),* (2013).
26. B. G. Bathula, R. K. Sinha, A. L. Chiu, M. D. Feuer, G. Li, S. L. Woodward, W. Zhang, R. Doverspike, P. Magill, and K. Bergman, "Constraint routing and regenerator site concentration in ROADM networks," IEEE/OSA J. Opt. Commun. Netw. **5**, 1202–1214 (2013).
27. T. Zami, "Multiflow application for WDM networks with multicarrier transponders serving superchannels in contentionless OXCS[invited]," IEEE/OSA J. Opt. Commun. Netw. **9**, A114–A124 (2017).
28. E. Agrell and M. Secondini, "Information-theoretic tools for optical communications engineers," in *2018 IEEE Photon. Conf. (IPC),* (2018).
29. L. M. Zhang and F. R. Kschischang, "Staircase codes with 6 % to 33 %

overhead," J. Light. Technol. **32**, 1999–2002 (2014).
30. P. K. Vitthaladevuni, M. . Alouini, and J. C. Kieffer, "Exact BER computation for cross QAM constellations," IEEE Trans. on Wirel. Commun. **4**, 3039–3050 (2005).